Design and development of a novel fused filament fabrication (FFF) 3D printed diffusion cell with UV imaging capabilities to characterise permeation in pharmaceutical formulations

Zayeem Fazili[a, b, c], Adam Ward[a], Karl Walton[b,c], Liam Blunt[b,c], Kofi Asare-Addo[a*]

[a]Department of Pharmacy, University of Huddersfield, Huddersfield, HD1 3DH, UK

[b]EPSRC Future Metrology Hub, University of Huddersfield, Huddersfield, HD1 3DH, UK

[c]Department of Computing and Engineering, University of Huddersfield, Huddersfield, HD1 3DH, UK

*Corresponding author (Kofi Asare-Addo)

E-mail: k.asare-addo@hud.ac.uk

Tel: +44 1484 472360

Fax: +44 1484 472182

Abstract

The present work aimed at designing and developing a novel 3D printed diffusion cell capable of UV imaging using the fused filament fabrication (FFF) method. UV imaging has proven to be very versatile in the area of pharmaceutics giving insights into various phenomena including the dissolution behaviour of dosage forms, intrinsic dissolution rates and the drug precipitation processes. A 3D printed diffusion cell in similitude of a Franz cell was successfully printed using polylactic acid (PLA) filaments equipped with quartz for the imaging area. A model ibuprofen (IBU) gel formulation was tested by introducing the dosage form through the 3D printed donor compartment and the drug concentration permeated through the skin mimic (silicone membrane) was determined from the 3D printed receptor compartment using UV imaging in real-time. The results showed successful UV imaging of the permeation of IBU gel in the novel diffusion cell potentially negating further analytical processes such as the HPLC process required for Franz cell tests thereby reducing costs. Potential interactions between the drug and filament used in the 3D printed process suggests although this concept can be moved towards commercialisation, care should be taken with choice of filament used in the 3D printing process.

Keywords

Fused filament fabrication (FFF); UV imaging; Permeation; Ibuprofen gel; 3D printing; Diffusion cell

1. **Introduction**

In vitro permeation tests are conducted to study a drugs release from a semisolid formulations. This is critical to monitor *in vivo* performance [1]. In contrast to other routes of drug administration such as oral delivery, transdermal methods of drug delivery are being progressively more researched due to its benefit of avoiding first pass metabolism and reduced toxicity [2] thereby improving patient compliance. The United States Pharmacopeia general chapter 1724 [3] details the Franz cell diffusion-based evaluation of a topical formulation. The Franz cell *in vitro* release testing method has proved an invaluable approach to quantify the drug release from semisolid formulations through transdermal administration. The assembly of the Franz cell can be broken down into two separate parts. The first part is named as a donor chamber, and the other termed as a receptor chamber. Both parts are typically manufactured from borosilicate glass. These two chambers are separated by a membrane which can be artificial (synthetic membrane) or skin (human or animal). The orifice diameter of the donor and the receptor chamber depends on the application and can have different sizes. The donor chamber is filled with the formulation (semisolid state drug) and spread evenly on the membrane surface. The formulation diffuses through the membrane into the receptor chamber usually containing a phosphate buffer as a release media. The capacity of the release media to dissolve drug should be sufficiently high to achieve the sink conditions [3]. Typically 200 mg - 400 mg of the dosage (gel or cream) is used for performance testing. However, increased amounts are detailed elsewhere [1, 4]. The cell is kept at a temperature of 37 °C during experiments by circulating 37 °C equilibrated water through a cell jacket to maintain membrane temperature [1, 3, 5-7]. A magnetic stirrer (usually Teflon coated) at the bottom of the cell ensures uniformity of the drug content in the receptor chamber consisting of the release media. The stirring magnetic speed is kept between 600 - 800 ± 10 % rpm [3]. The typical sampling interval is 1 h ± 2 min over a range of 4, 6, 12, 24 & 72 h. At each sampling interval the receptor chamber is refilled with the same amount of volume taken for sampling with fresh media [1, 3-7]. This traditional permeation quantification method requires manual measurements of the small test samples from the bulk solution through a UV spectrophotometry technique usually HPLC. This can be labour intensive and prone to human errors. There is thus a need for real-time monitoring methodologies that can determine and provide insights into the permeation events more precisely and autonomously.

A second generation surface dissolution imaging instrument (SDi2) is used in the determination of the UV imaging aspects of the present study. Østergard et al. [8] first investigated nicotine

release from a transdermal patch using UV imaging [8]. The authors investigated the real-time formation of concentration gradients to evaluate the quantitative advocacy of the UV imager. Ye et al. [9] showed the potential of the UV imaging technique in studying diffusion in hydrogels. The authors successfully investigated the diffusion of human serum albumin and piroxicam in Pluronic F127 hydrogels where a phosphate buffer was used as a release medium. The same authors also developed a non-intrusive model to study the drug release through subcutaneous means [10]. Gaunø et al. [11] also successfully established a UV imaging technique to monitor the *in vitro* release of 5-aminosalicylic acid extrudate coated with ethyl cellulose film placed in the agarose gel. Several other authors have also utilised the UV imaging platform to determine intrinsic dissolution rates of active pharmaceutical ingredients (API), characterisation of salts, cocrystals, solid dispersions and in quality control assessments [12-32]. The aforementioned studies have thus proved useful in establishing UV imaging for drug and formulation characterisation and therefore is the author's rationale for using this as a platform to develop a UV imaging setup which can facilitate real-time characterisation of APIs in transdermal drug administration.

3D printing or additive manufacturing has revolutionised product development and prototyping. 3D printing has proved to be a versatile manufacturing tool given the flexibility and ease of manufacturing whilst being substantially cost efficient. The availability of 3D printing technologies include stereolithographic, powder bed based, selective laser sintering, fused filament fabrication, semi-solid extrusion and powder bed inkjet printing [33, 34] with commercially available filaments such as PVA, acrylonitrile butadiene styrene (ABS) and PLA often used [35]. With regards to the development of the transdermal *in vitro* testing systems, Sil et al. [36] successfully developed and tested a 3D transparent traditional Franz cell with Suarato et al. [37] also successfully developing and testing a pocket-sized diffusion cell for skin permeation. Ding et al. [38] also successfully developed a miniaturised device in the bid for reducing the amount of skin sample required for permeation studies using 3D printing.

In this study, a proof of concept cost effective novel 3D printed diffusion cell in the similitude of a Franz cell is defined that allows non-intrusive real time UV imaging across synthetic membranes to characterise the permeation of a topical formulation. As well as the UV imaging aspects of the developed 3D printed cell, the presented work also seeks to extract quantitative data from the generated images in a bid to reduce the labour intensive and potential costs that can be associated to further analytical tests with the traditional Franz cell.

2. Materials and Methods

2.1. Materials

Ibuprofen was purchased from TCI Chemicals Ltd, Oxford, UK. A 5 % w/w ibuprofen gel formulation was used as the model topical formulation. A 100 g tube of the gel was purchased from Vivomed, Downpatrick, UK. Phosphate buffer (pH 7.2) was used as the release media in the receptor compartment and was prepared using sodium hydroxide and potassium phosphate monobasic purchased from Fisher Scientific Ltd, Loughborough, UK and Acros Organics, Germany, respectively. Silatos™ silicone membrane of thickness 0.13 mm was purchased from Atos Medical, Sweden. 40 mm × 40 mm × 10 mm (H × L × W) three-pin fan and two circular neodymium magnets of size 2 mm × 2 mm (H × D) were purchased from Amazon Ltd, UK. A magnetic stirrer bar of diameter 4 mm and length 15 mm was purchased from Fisher Scientific Ltd, Loughborough. Loctite® super glue was purchased from Amazon Ltd, UK. NZXT Sentry 3 Fan Controller and GELID system fan speed controller were purchased from Amazon Ltd, UK. A tachometer was also purchased from Amazon Ltd, UK to measure the rpm of the magnetic stirrer bar. A 3D printing filament PLA (polylactic acid) was purchased from Technology Outlet Ltd, Leicestershire, UK. The parts were printed with the RAISE3D N2 printer purchased from RAISE3D, Rotterdam, Netherlands. Two 30 mm × 30 mm ×1 mm (H × L × W) fused silica quartz windows were purchased from Galvoptics Ltd, Basildon, UK. Opti-tec 5001 optical epoxy adhesive was purchased from Intertonics Ltd, Oxfordshire, UK. A 62.16 mm × 9.06 mm × 5.86 mm (H × L × W) quartz dose tube was purchased from Pion Inc. Ltd, Essex, UK.

2.2. Methods

2.2.1. CAD Model and drawings

A prototype diffusion cell in the similitude of a Franz cell was designed in SolidWorks® (2018). A dose-controlled tube and a membrane aligner were also designed. A lid was designed to allow insertion of the dose tube. Figure 1 depicts the 3D CAD model of the cell. For securing the diffusion cell in the surface dissolution instrument (SDi2) UV system, a stand was designed. During the designing process, it was necessary to design a stand to the dimensions which would allow sufficient height for the diffusion cell window to align correctly and at the right position with the CMOS detector inside the SDi2 UV system. Figure 2 depicts a 3D CAD model of the stand.

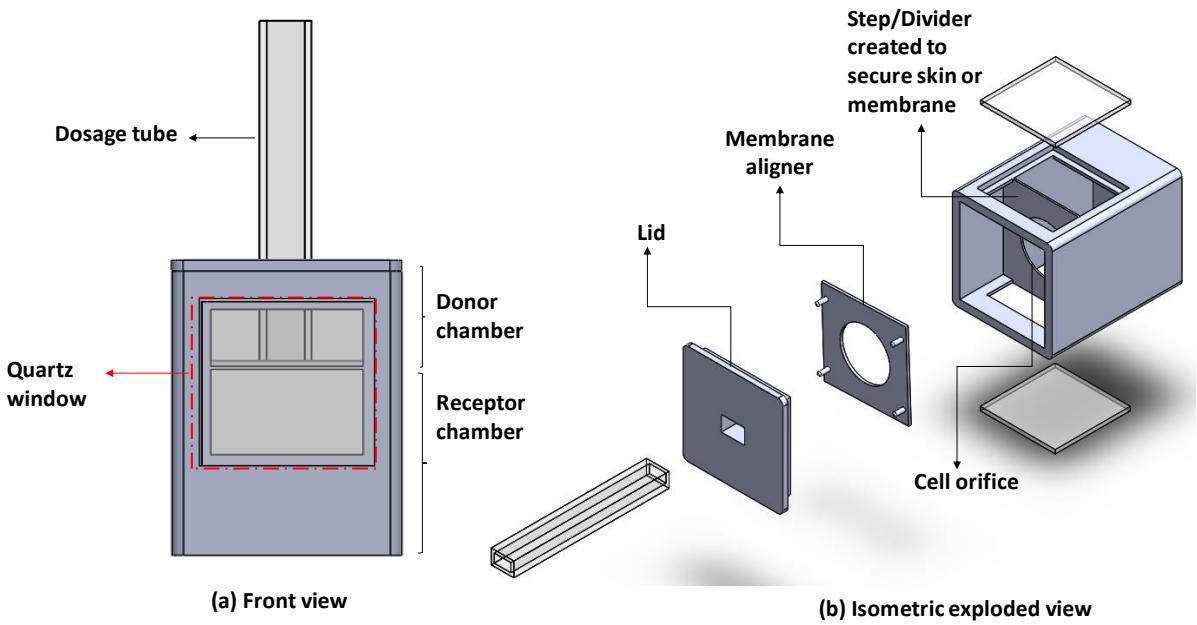

154

155 Figure 1. 3D CAD model (a) Front view of the 3D printed diffusion cell prototype with dosage
156 tube inserted from the top (b) Isometric exploded view of the prototype.

157

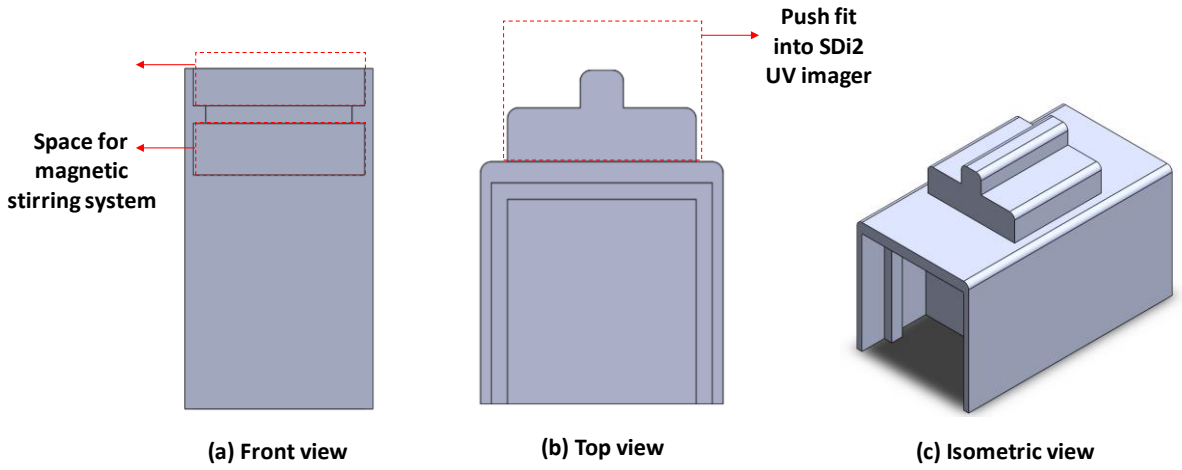

158

159 Figure 2. 3D CAD model (a) Front view (b) Top view (c) Isometric view of the stand designed
160 to secure the 3D printed diffusion cell in SDi2 UV system.

161

162 *2.2.2. Manufacturing Franz cell and the stand.*

163 The CAD files of the diffusion cell, membrane aligner, lid and the diffusion cell stand were
164 converted to STL files in SolidWorks® (2018). The STL files were post-processed in the 3D
165 printing software, Slicer. The 3D printing filament PLA (polylactic acid) was used to print the
166 required parts. The parts were printed with the RAISE3D N2 printer. The printer nozzle

temperature was set at 220 °C and the printer bed temperature was set at 50 °C. The speed of the nozzle was set at 65 mm/s. The layer height was set at 0.2 mm. The parts were printed with 2 shells (each shell was 0.4 mm thick). The infill was set at 30 %. The diffusion cell was printed with the following specifications: 52 mm × 40 mm × 40 mm (H × L × W) volume of receptor compartment was 30 mL ± 1 mL and the volume of the donor compartment was 20 mL ± 1 mL. The orifice area was 3.14 cm^2 ± 0.2. The diffusion cell stand was printed with following specifications: 82.10 mm × 45 mm × 45 mm (H × L × W). After the cell was manufactured, two 30 mm × 30 mm ×1 mm (H × L × W) fused silica quartz windows were bonded to the cell by using Opti-tec 5001 optical epoxy adhesive. The optical path length was approximately 40 mm between the two quartz windows of the diffusion cell. A quartz dosage tube was inserted into the cell through the lid.

2.2.3. Magnetic stirrer

There are a variety of magnetic stirring systems of different sizes available commercially however these are significantly too large to fit into the SDi2 UV imager. To address this challenge, a customised magnetic stirring system was built for the designed prototype diffusion cell. The customised magnetic stirring system was developed from a computer CPU cooling fan and neodymium magnets. Neodymium magnets were bonded to the centre of the fan with superglue, and the fan was inserted into the 3D printed diffusion cell stand.

2.2.4. UV Calibration using SDi2

To calibrate the diffusion cell, a series of standards for IBU were produced. Each series of standards was made from a 1 mg/mL stock solution of IBU produced by adding 100 mg of ibuprofen to 100 mL volumetric flasks and making to volume using the phosphate buffer. Three stock solutions were prepared and labelled as A, B and C. Twenty-one standards (7 from A, 7 from B and 7 from C) were prepared using concentration ranges from 10 – 200 µg/mL using 100 mL volumetric flasks. Once all the standards were prepared, they were placed in a water bath at a 37 °C and allowed to equilibrate. The 3D printed diffusion cell absent of any liquid was then placed in the SDi2 system (Figure 3) with the magnetic stirring system switched off.

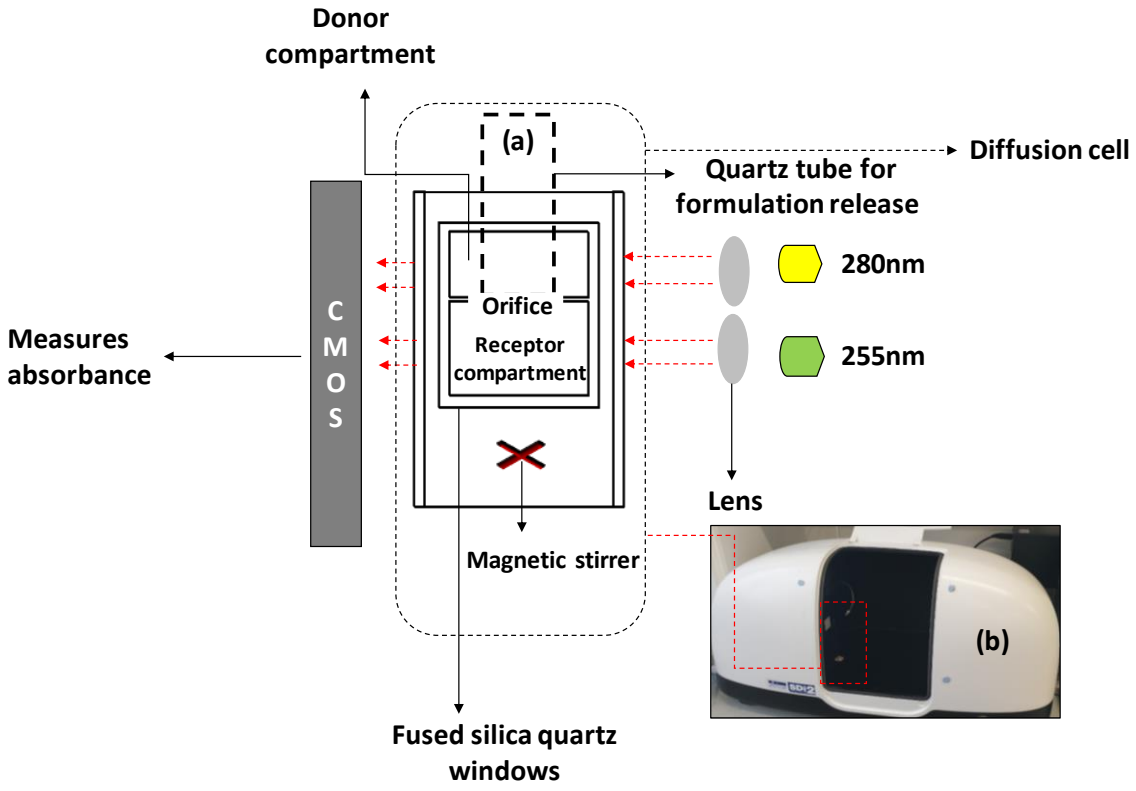

197

198 Figure 3. (a) Schematic of the setup used to calibrate the 3D printed diffusion cell prototype
199 for IBU (b) SDi2 UV system in which the 3D printed diffusion cell is placed

200

201 A measuring zone as depicted in Figure 4 was set using the analysis software supplied with the
202 SDi2 system to extract data for the calibration curve. The data analysis method consisted of 5
203 min intervals, each separated by 2 min intervals to allow for sample change. The system was
204 also set to maintain at 37 °C and to record UV absorbance of IBU at 255 nm and 280 nm. The
205 closest LED (255 nm) was selected for data analysis due to IBU's lambda max [39].

206

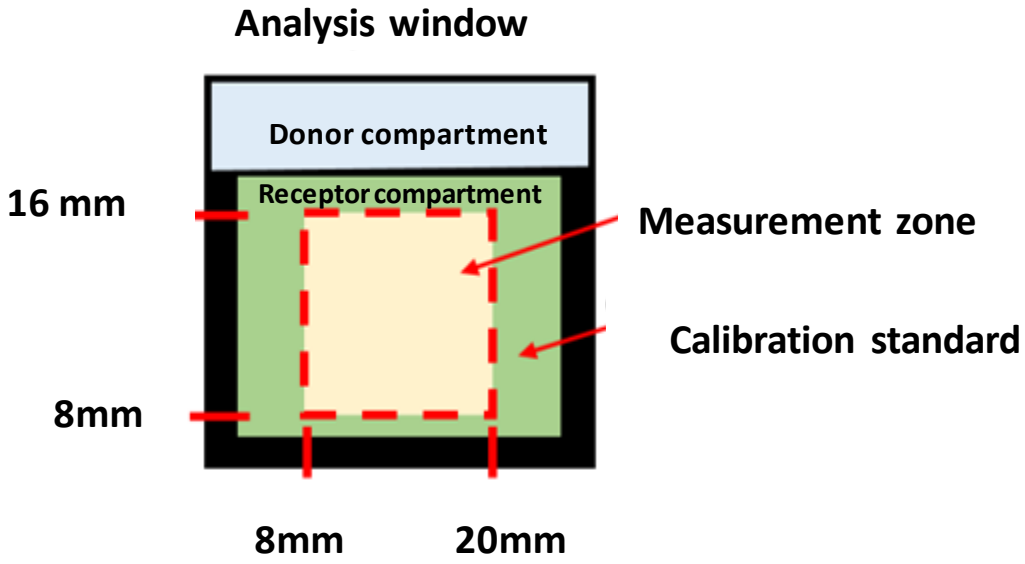

207

208 Figure 4. Schematic of a set measurement zone for extracting absorbance data to calibrate the
209 3D printed diffusion cell prototype.

210

211 *2.2.5. Membrane preparation*

212 Before analysis of the ibuprofen gel using the 3D printed diffusion cell, the 0.13 mm thick
213 silicone membrane was prepared. Firstly, a 20 × 20 mm (H × L) square of the membrane was
214 cut and placed in a glass beaker. Next, approximately 40 mL of phosphate buffer pH 7.2 was
215 added to the beaker. The beaker containing the membrane and buffer was then placed in a sonic
216 bath for 10 min to degas and then placed in a water bath at 37 °C to equilibrate for another 20
217 min.

218

219 *2.2.6. UV imaging of the permeation process*

220 Before the assessment, the lower receptor compartment of the cell was filled with degassed
221 phosphate buffer (pH 7.2) using a syringe until the cell receptor chamber was filled up to the
222 orifice (approximately 30 mL of buffer was found to be held by the cell receptor cell). The
223 silicone membrane of thickness 0.13 mm was placed on a divider between the donor and
224 receptor compartments providing a diffusion area of 3.14 cm^2. The membrane was sandwiched
225 between the aligner and the 3D printed diffusion cell divider. A method was constructed using
226 the SDi2 data collection software to record data using the 255 nm and 520 nm (Vis) LEDs to
227 quantify drug absorbance and to track possible gel movements respectively. The cell was

secured in the SDi2 UV imager to blank the system for setting a benchmark value for the UV absorbance. After the blanking process, the donor compartment of the cell was filled with approximately 1 mL of the IBU gel administered by filling the quartz tube with a 5 mL syringe. The whole assembly containing the IBU gel was placed in the SDi2 UV imager such that the interface between the membrane and receptor compartment and the interface between the membrane and IBU gel aligned in a straight path between the UV LEDs and the CMOS chip (Figure 5). The magnetic stirring system was turned on and the speed set to 600 rpm with the fan controlling system. The experiment was conducted for 12 h in triplicate at 37 °C.

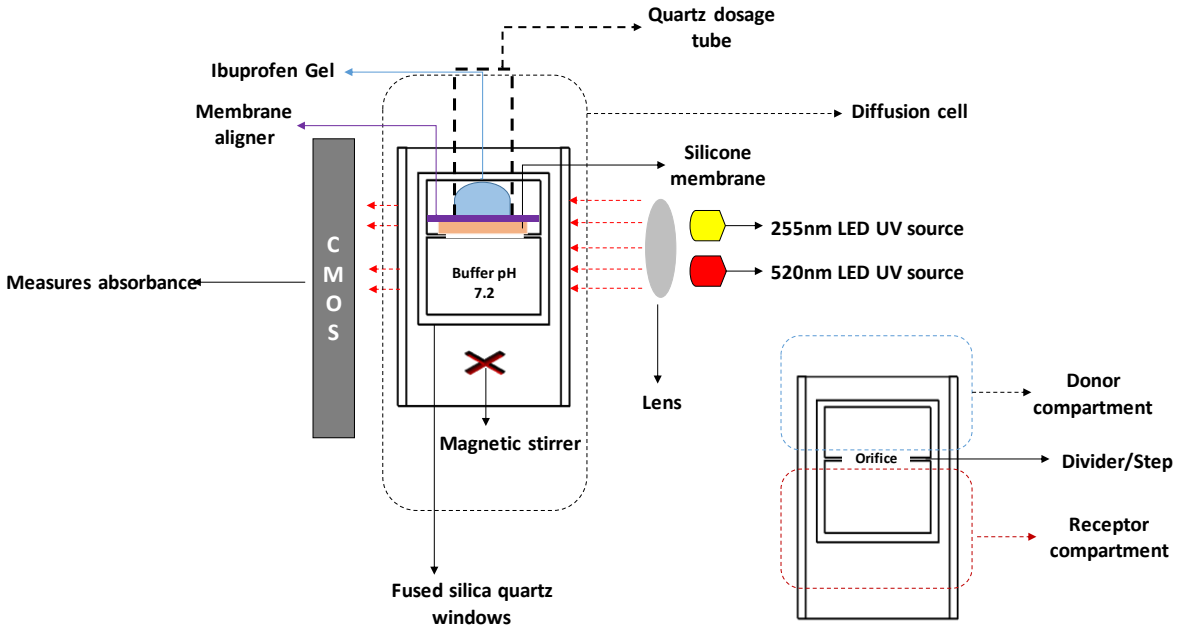

Figure 5. Schematic of the setup to quantify the amount of IBU permeating through a silicone membrane.

The analysis software supplied with the SDi2 system was used to set up a measuring zone to extract the permeation data (Figure 6). The absorbance readings at 30 s intervals were extracted from the software. The raw data was processed using Microsoft Excel™ and the calibration curve to provide a quantitative assessment of IBU permeated through the membrane.

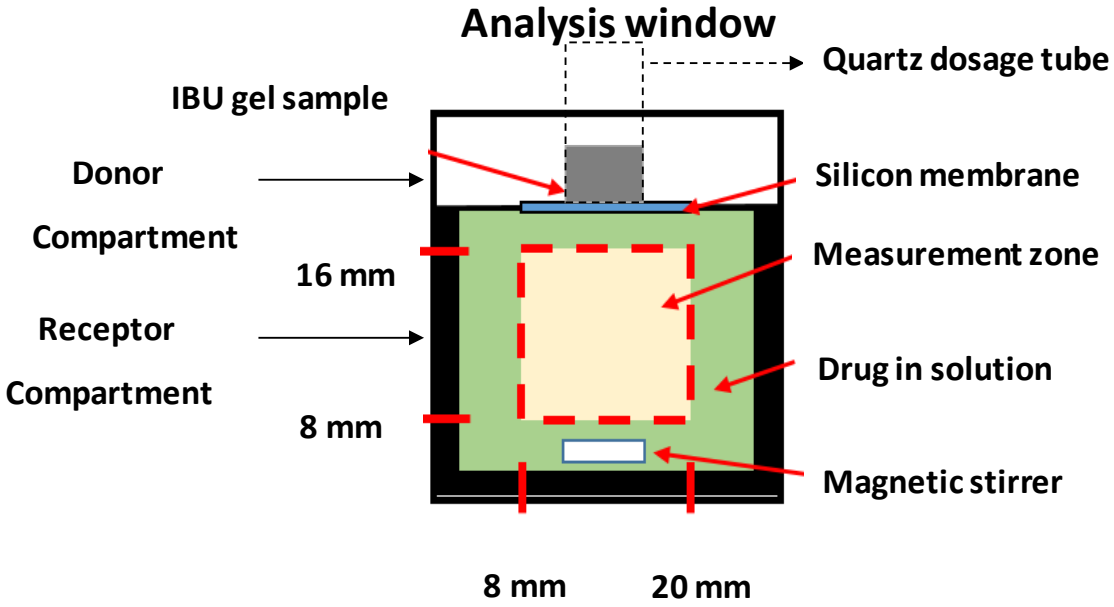

Figure 6. Schematic of a set measurement zone for extracting absorbance data for the 3D printed diffusion cell prototype for IBU permeation analysis

3. Results and discussion

3.1. Fabrication of the 3D printed diffusion cell

Figure 7 depicts the successfully manufactured 3D printed diffusion cell. Figure 7a depicts the aligner that is important in keeping the membrane of interest taut. Figure 7b depicts the quartz dose tube in which the formulation of interest is decanted and Figure 7c displays the full assembled unit with the 3D printed diffusion cell sat on top of the 3D printed stand that secures the whole unit for the UV imaging process. The 3D printed diffusion cell system aligned well with the imaging process. The red dashed line in Figure 1a depicts the area available for UV imaging in the developed diffusion cell.

As a Franz cell requires a stirring capability to continuously agitate the release media in the receptor chamber to achieve uniformity in the solution during an *in vitro* drug release test, a clearance (indicated by a red arrow on Figure 7c) was left in the stand for incorporating a magnetic stirring system which would facilitate stirring of a magnetic bar placed in the receptor chamber of the 3D printed diffusion cell (Figure 8). Figure 8a depicts the custom developed magnetic stirrer used to achieve stirring conditions in the manufactured 3D printed diffusion cell with the red dashed circle indicating the location of the glued neodymium magnets. Figure

8b shows the fully assembled unit with the stirring insert. The stirring system was powered by a NZXT Sentry 3 Fan Controller embedded in the CPU of the SDi2 system. Figure 8c shows the location of the magnetic stirrer (red dashed circle) within the receptor compartment of the 3D printed diffusion cell. The minimum rpm achieved with NZXT Fan controller was about 1000 rpm and was displayed by the screen of NZXT Fan controller. This was manually confirmed by measuring with tachometer. The speed obtained (1000 rpm) was significantly above that prescribed for the Franz cell (600 - 800 rpm) as recommended by USP 1724 [3]. A GELID system fan speed controller was thus connected between the fan with magnets (stirring system) and the fan controller fitted in the SDi2 CPU to overcome this challenge. Using the GELID system fan speed, the rpm was controlled between 0 - 2500 rpm max. The sequence of connections used is detailed in achieving this is depicted in Figure 9.

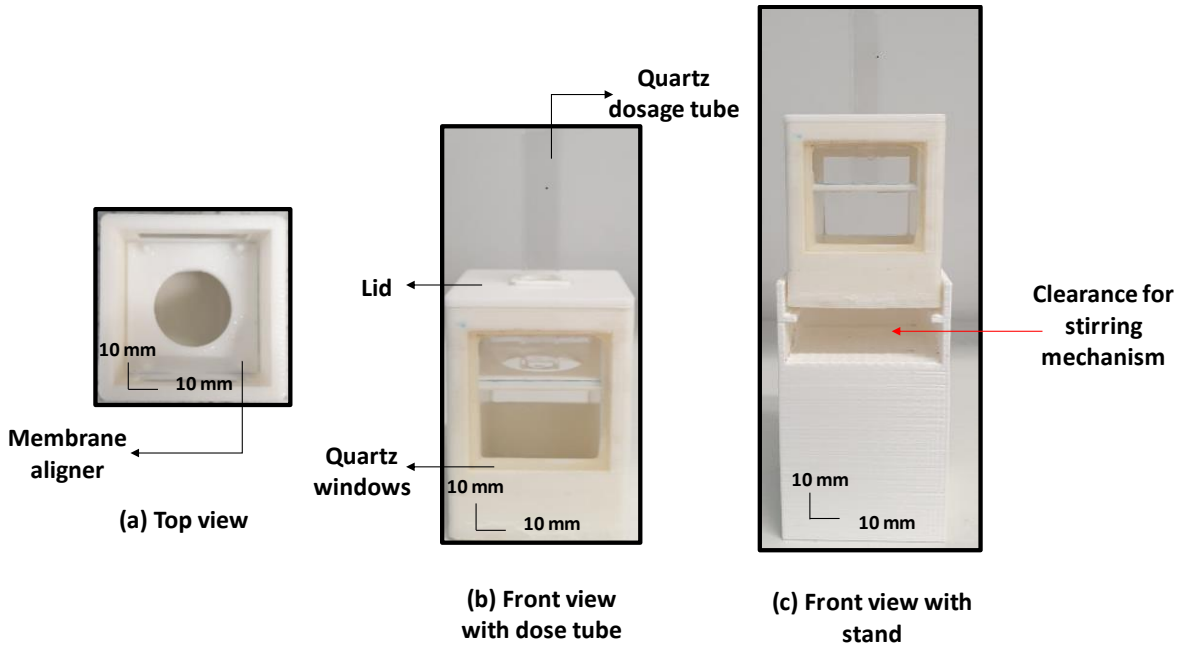

Figure 7. Assembled 3D printed diffusion cell prototype. Image shows (a) Top view of the cell without the lid showing a membrane aligner inside (b) 3D printed diffusion cell with bonded quartz windows & a quartz dosage tube inserted from the top (c) Front view of the cell secured on the 3D printed stand.

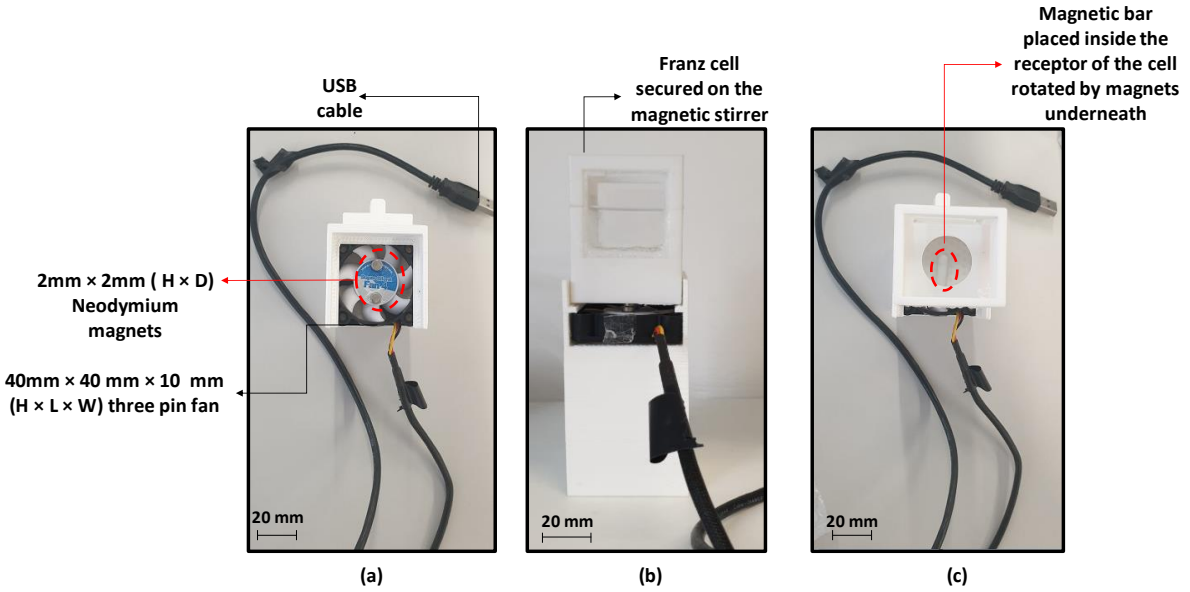

Figure 8. (a) Custom developed magnetic stirrer for the Franz cell. Image shows a) 40 mm × 40 mm × 10 mm (H × L × W) three-pin computer fan with bonded 2 mm × 2 mm (H × D) secured inside the 3D printed diffusion cell stand (b) 3D printed diffusion cell secured on the magnetic stirrer c) A Teflon magnetic stirrer bar of diameter 4 mm and length 15 mm placed inside the receptor chamber of the 3D printed diffusion cell.

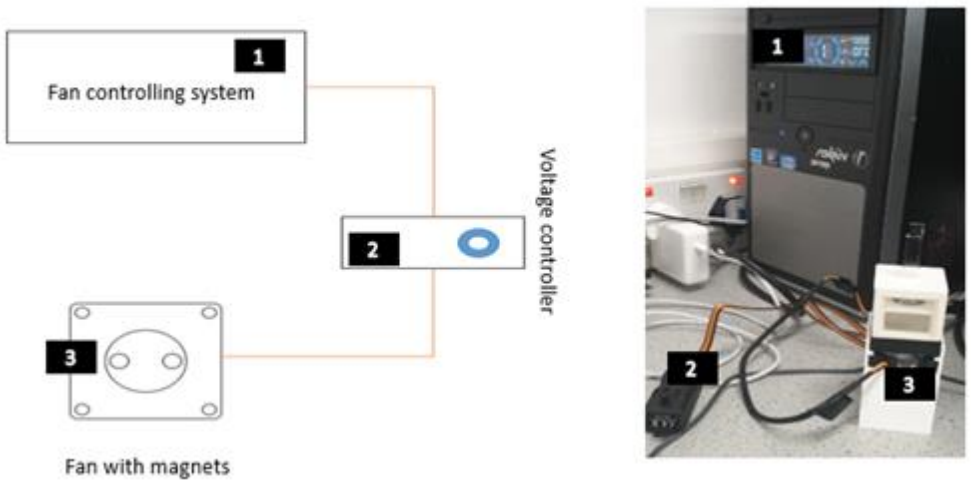

Figure 9. Images on the left depict a schematic circuit of a magnetic stirring controlled system used in 3D printed diffusion cell prototype and images on the right image shows the actual connections.

3.2. Assessing the UV permeation capabilities of the 3D printed diffusion cell

The absorbance readings at 30 s intervals were extracted from the software and the extracted data was plotted using Microsoft Excel™ to produce a calibration curve for the IBU standards of stock A, B and C. The average calibration profile of all stocks (A, B & C) is depicted as Figure 10a with its accompanying UV images (Figure 10b). The time points on the calibration curve (Figure 10a) are also colour coded to match its corresponding UV images (Figure 10b). The generated calibration curve had an r^2 value of 0.9931 which is an indication of linearity. The derived equation (Figure 10a) was used in determining the concentration of the permeated IBU in the receptor chamber.

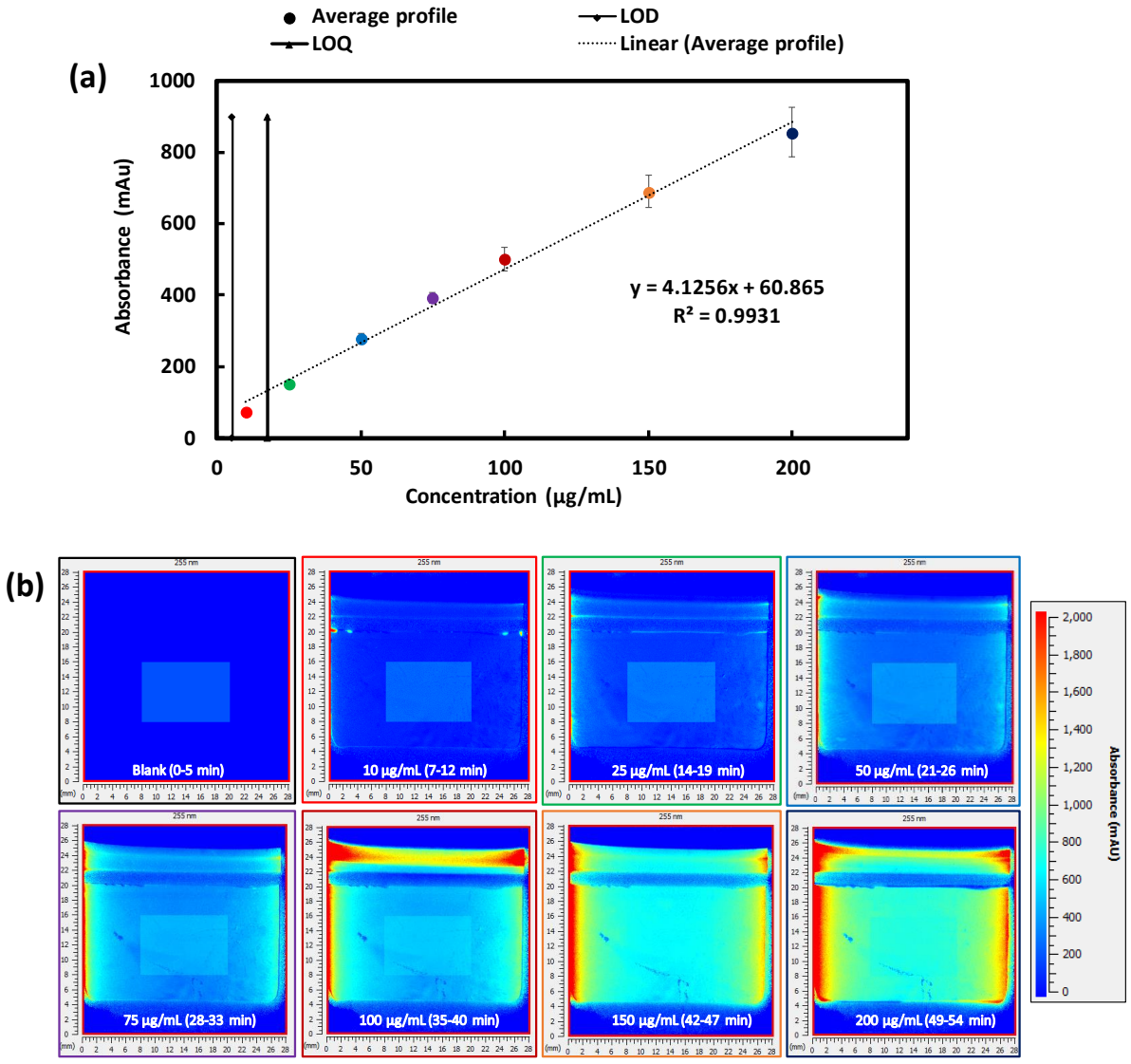

Figure 10. (a) Average IBU calibration curve of stock A, B & C with a limit of detection & quantification. Coloured points correlate with images from Figure 10b (b) UV images at 255

nm generated from a series of standards prepared from IBU to calibrate the 3D printed diffusion cell. Images colour coded with reference to Figure 10a.

The function of the membrane aligner (Figure 7a) was to prevent the formation of slack in the membrane due to the IBU gel (formulation) weight. The quartz dose tube was also introduced to avoid the uneven spread of gel over the membrane. The 3D printed diffusion cell proved useful in allowing the visualisation of the permeation process as well as determining the quantification of IBU permeating through the silicon membrane. The amount of IBU permeated through the silicon membrane was quantified by converting milli absorbance units (mAu) into concentration (µg/mL) using the linear calibration equation (Figure 10a). The average permeation profile achieved for triplicate run over a 12 h period is shown in Figure 11a. Figure 11a suggests the concentration of the IBU drug from the gel formulation gradually increased over 12 h without reaching a plateau state within this time frame (12 h). This indicated a longer run time might be needed for observation of a plateau state. Figure 11a also suggests data points between 0 - 25 min fall below the limit of quantification (17.69 µg/mL) which was determined. This undermines the reliability of the data at these points. It was also observed from Figure 11a that the data set between 420 min - 720 min exceeded the limit of 200 µg/mL which was the highest standard used to calibrate the cell (Figure 10) (this suggested mAUs above 900 to not be reliable), thus indicating data between 440 min - 720 min may also not be reliable due to potential deviations from linearity and potential issues of over-saturation of the detector as a result of sink conditions. This oversaturation of the detector was observed also by Ward et al when obtaining a calibration for propranolol hydrochloride (31). The higher absorbance readings towards the edges of the images at around 2000 mAu in Figure 11b and also observed during the calibration process (Figure 10b) may also be due to possible interactions or drug diffusing through the walls of the filaments used in the 3D printing process of the 3D printed diffusion cell all of which have to be investigated further. Several authors have utilised the ability of drugs to diffuse through filaments for the 3D printing of medicines (40-42) although PVA polymers were used. It is therefore of importance to print these diffusion cells with filaments that do not interact with or allow drug permeation into them. It is also important to note that PLA is hydrolytically degraded over time (hydrolytic chain scission during which polymer chains are cleaved into oligomers and finally monomers) (43). This therefore makes it difficult to predict the number of times the diffusion cell could be used accurately before errors could occur. Also the use of solvents such as acetone, ester and chloride solvents have been reportedly used as chemical finishing for 3D printed materials (44, 45). It is therefore

important that such solvents are not used in the cleaning process as they could affect the integrity of the cell. Exposure to media for lengthy periods of time (potential imbibement of media) and the drying process could affect the cell integrity also. To significantly reduce errors, care was taken with the experimentations and deionised water was only used for the cleaning process and the printed cell was air dried at room temperature. It is therefore important that if PLA is being used as the polymer of choice for printing the diffusion cell that care and consideration is given to the issues discussed above to ensure errors are not introduced. The use of such novel diffusion cells however have the potential capability of reducing the need for further analytic techniques such as HPLC thereby making it cost effective.

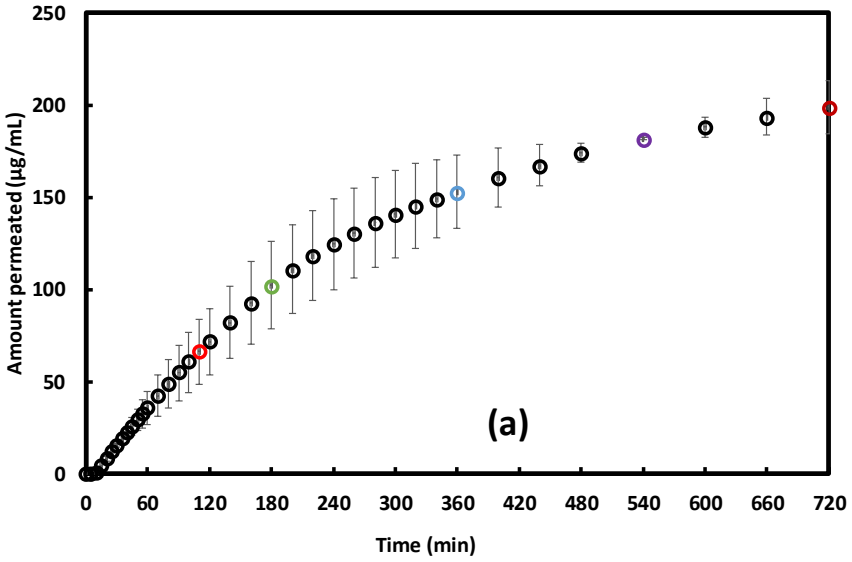

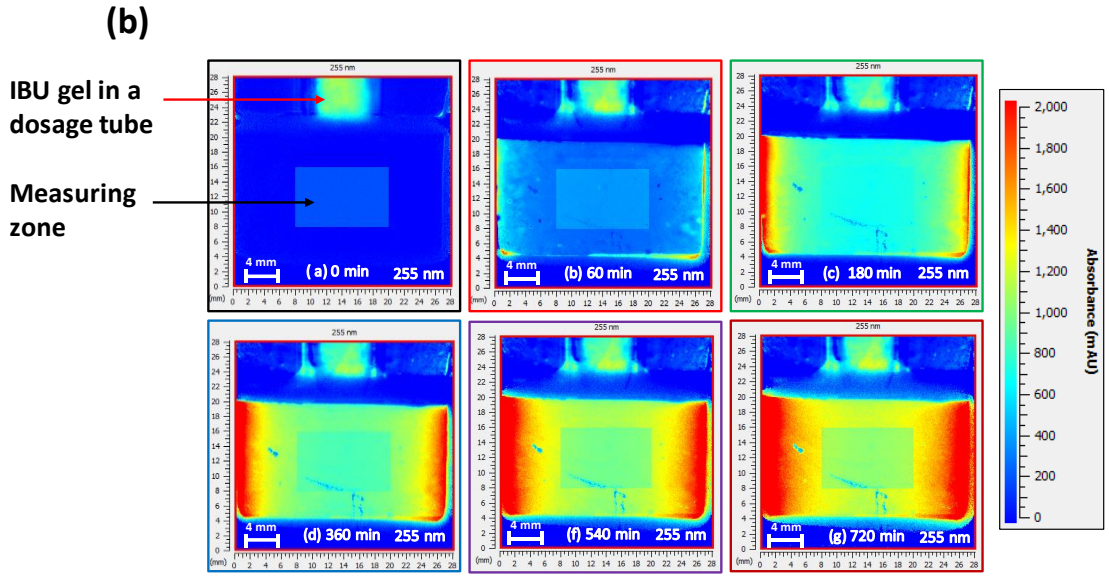

Figure 11. (a) Average IBU amount in µg/mL permeated vs time. Coloured points correlate with images from Figure 11b (b) UV images of the 3D printed diffusion cell's IBU permeation at 255 nm. Images colour coded with reference to Figure 11a.

4. Conclusion

FFF was successfully used in manufacturing a permeation cell that was capable of UV imaging the drug permeation process of a topical semi-solid dosage form through a silicone membrane. This novel 3D printed permeation cell facilitated real-time UV characterisation of IBU permeation from a model topical formulation. This process eliminated the use of further instrumentation such as HPLC for the drug quantification process. Although this system provides a quick and user friendly way of capturing data, it is important to note that issues such as the nature of the filament used in the printing process of such diffusion cells that ensures no drug leakages into the filaments or possible interactions need are addressed. This as well as the ability of producing data that can match the traditional Franz cell and its hydrodynamics are of great importance and the subject of further studies.

Acknowledgements

Zayeem Fazili thanks the University of Huddersfield for the proof of concept funding received for this work. The authors also thank Karl Box, Hayley Watson and Becky Upton of Poin Inc and Mark Vaux and David Goodall of Paraytec Limited for their insights and discussions on UV imaging.

Conflict of interest

The authors have applied for a patent for this novel diffusion cell (patent application number GB1913709.0)

Author contributions

Zayeem Fazili: Conceptualization; Data curation; Formal analysis; Writing; **Adam Ward**: Conceptualization; Data curation; Formal analysis; **Karl Walton**: Supervision; Funding acquisition; Resources; Writing - review & editing; **Liam Blunt**: Supervision; Funding acquisition; **Kofi Asare-Addo**: Funding acquisition; Supervision; Investigation; Methodology; Project administration; Resources; Supervision; Validation; Visualization; Roles/Writing - original draft; Writing - review & editing.

383

384

385 References

386 [1] C. T. Ueda, V. P. Shah, K. Derdzinski, G. Ewing, G. Flynn, H. Maibach, et al. Topical and
387 transdermal drug products. Dissolution Technologies. 2010;17(4):12-25.

388 [2] J. Ostergaard. UV imaging in pharmaceutical analysis. J Pharm Biomed Anal.
389 2018;147:140-8.

390 [3] United States Pharmacopeial C, United States Pharmacopeial Convention. Council of E.
391 The United States pharmacopeia [and] The national formulary, 2019: Volumes 1-5. USP: forty-
392 second revision ; NF: thirty-seventh ed. Rockville, Maryland: United States Pharmacopeial
393 Convention; 2018.

394 [4] C. H. Salamanca, A. Barrera-Ocampo, J. C. Lasso, N. Camacho, C. J. Yarce. Franz diffusion
395 cell approach for pre-formulation characterisation of ketoprofen semi-solid dosage forms.
396 Pharmaceutics. 2018;10(3):148.

397 [5] T. Uchino, F. Lefeber, G. Gooris, J. Bouwstra. Characterization and skin permeation of
398 ketoprofen-loaded vesicular systems. European Journal of Pharmaceutics and
399 Biopharmaceutics. 2014;86(2):156-66.

400 [6] S. J. Gallagher, L. Trottet, C. M. Heard. Ketoprofen: release from, permeation across and
401 rheology of simple gel formulations that simulate increasing dryness. International Journal of
402 Pharmaceutics. 2003;268(1):37-45.

403 [7] Y. S. Rhee, J.G. Choi, E.S. Park, S.C. Chi. Transdermal delivery of ketoprofen using
404 microemulsions. International Journal of Pharmaceutics. 2001;228(1):161-70.

405 [8] J. Østergaard, E. Meng-Lund, S. W. Larsen, C. Larsen, K. Petersson, J. Lenke, et al. Real-
406 Time UV Imaging of Nicotine Release from Transdermal Patch. Pharmaceutical Research.
407 2010;27(12):2614-23.

408 [9] F. Ye, A. Yaghmur, H. Jensen, S. W. Larsen, C. Larsen, J. Østergaard. Real-time UV
409 imaging of drug diffusion and release from Pluronic F127 hydrogels. European Journal of
410 Pharmaceutical Sciences. 2011;43(4):236-43.

[10] F. Ye, C. Larsen, S. W. Larsen, A. Yaghmur, H. Jensen, J. Østergaard. Real-time UV imaging of piroxicam diffusion and distribution from oil solutions into gels mimicking the subcutaneous matrix. European Journal of Pharmaceutical Sciences. 2012;46(1-2):72-8.

[11] M. H. Gaunø, T. Vilhelmsen, C. C. Larsen, J. P. Boetker, J. Wittendorff, J. Rantanen, et al. Real-time in vitro dissolution of 5-aminosalicylic acid from single ethyl cellulose coated extrudates studied by UV imaging. Journal of Pharmaceutical and Biomedical Analysis. 2013;83:49-56.

[12] M. Kuentz, (2015). Analytical technologies for real-time drug dissolution and precipitation testing on a small scale. Journal of Pharmacy and Pharmacology, 67(2), 143-159.

[13] K. Asare-Addo, M. Alshafiee, K. Walton, A. Ward, A. Totea, S. Taheri, . . . B. R. Conway, (2019). Effect of preparation method on the surface properties and UV imaging of indomethacin solid dispersions. European Journal of Pharmaceutics and Biopharmaceutics, 137, 148-163. doi:10.1016/j.ejpb.2019.03.002

[14] J.P. Boetker, J. Rantanen, T. Rades, A. Mullertz, J. Ostergaard, H. Jensen, (2013). A new approach to dissolution testing by UV imaging and finite element simulations. Pharmaceutical Research, 30(5), 1328-1337. doi:10.1007/s11095-013-0972-0

[15] J. P. Boetker, M. Savolainen, V. Koradia, F. Tian, T. Rades, A. Müllertz, . . . J. Østergaard, (2011). Insights into the early dissolution events of amlodipine using UV imaging and raman spectroscopy. Molecular Pharmaceutics, 8(4), 1372-1380. doi:10.1021/mp200205z

[16] A. Ward, K. Walton, K. Box, J. Ostergaard, L. J. Gillie, B. R. Conway & K. Asare-Addo, (2017). Variable-focus microscopy and UV surface dissolution imaging as complementary techniques in intrinsic dissolution rate determination. International Journal of Pharmaceutics, 530(1-2), 139-144. doi:10.1016/j.ijpharm.2017.07.053

[17] K. Asare-Addo, K. Walton, A. Ward, A. M. Totea, S. Taheri, M. Alshafiee,. . . P. Timmins, (2018). Direct imaging of the dissolution of salt forms of a carboxylic acid drug. International Journal of Pharmaceutics, 551(1-2), 290-299. doi:10.1016/j.ijpharm.2018.09.048

[18] A. Ward, K. Walton, N. Mawla, W. Kaialy, L. Liu, P. Timmins, . . . K. Asare-Addo, (2019). Development of a novel method utilising dissolution imaging for the measurement of swelling behaviour in hydrophilic matrices. International Journal of Pharmaceutics: X, 1, 100013. doi:10.1016/j.ijpx.2019.100013

[19] L.H. Nielsen, S. Gordon, J.P. Pajander, J. Østergaard, T. Rades, A. Müllertz, (2013). Biorelevant characterisation of amorphous furosemide salt exhibits conversion to a furosemide hydrate during dissolution Int. J. Pharm., 457, pp. 14-24, 10.1016/j.ijpharm.2013.08.029

[20] J. Østergaard, (2018). UV imaging in pharmaceutical analysis. Journal of pharmaceutical and biomedical analysis, 147, 140-148.

[21] W. L. Hulse, J. Gray, R. T. Forbes, (2012). A discriminatory intrinsic dissolution study using UV area imaging analysis to gain additional insights into the dissolution behaviour of active 200 pharmaceutical ingredients. Int J Pharm 434:133–139.

[22] C. M. Long, K. Tang, H. Chokshi, & N. Fotaki, (2019). Surface Dissolution UV Imaging for Investigation of Dissolution of Poorly Soluble Drugs and Their Amorphous Formulation. AAPS PharmSciTech, 20(3), 113.

[23] P. Madelung, P. Bertelsen, J. Jacobsen, A. Müllertz, J. Østergaard, (2017). Dissolution enhancement of griseofulvin from griseofulvin-sodium dodecyl sulfate discs investigated by UV imaging. Journal of Drug Delivery Science and Technology, 39, 516. doi:10.1016/j.jddst.2017.05.010

[24] N. Qiao, K. Wang, W. Schlindwein, A. Davies, M. Li, (2013). In situ monitoring of carbamazepine–nicotinamide cocrystal intrinsic dissolution behaviour. European Journal of Pharmaceutics and Biopharmaceutics, 83(3), 415-426. doi:10.1016/j.ejpb.2012.10.005

[25] A. Niederquell, & M. Kuentz . Biorelevant dissolution of poorly soluble weak acids studied by UV imaging reveals ranges of fractal-like kinetics. International Journal of Pharmaceutics, 2014;463(1), 38-49. doi:10.1016/j.ijpharm.2013.12.049

[26] S. Colombo, M. Brisander, J. Haglöf, P. Sjövall, P. Andersson, J. Østergaard, M.Malmsten. Matrix effects in nilotinib formulations with pH-responsive polymer produced by carbon dioxide-mediated precipitation Int. J. Pharm., 494 (1) (2015), pp. 205-217

[27] S. Gordon, K. Naelapää, J. Rantanen, A. Selen, A. Müllertz, J. Ostergaard. Real-time dissolution behavior of furosemide in biorelevant media as determined by UV imaging

Pharm. Dev. Technol., 18 (2013), pp. 1407-1416, 10.3109/10837450.2012.737808

[28] Y. Sun, A. Chapman, S. W. Larsen, H. Jensen, N. J. Petersen, D. M. Goodall, & J. Østergaard, (2018). UV–vis Imaging of Piroxicam Supersaturation, Precipitation, and Dissolution in a Flow-Through Setup. Analytical chemistry, 90(11), 6413-6418.

[29] C. A. Bergström, K. Box, R. Holm, W. Matthews, M. McAllister, A. Mullertz, ... & A. Teleki, (2019). Biorelevant intrinsic dissolution profiling in early drug development: Fundamental, methodological, and industrial aspects. European Journal of Pharmaceutics and Biopharmaceutics

[30] F. Alqahtani, P. Belton, A. Ward, K. Asare-Addo, S. Qi (2020). An investigation into the use of low quantities of functional additives to control drug release from hot melt extruded solid dispersions for poorly soluble drug delivery. International Journal of Pharmaceutics, Available online 22 February 2020, 119172 https://doi.org/10.1016/j.ijpharm.2020.119172

[31] A. Ward, K. Walton, S. Stoycheva, M. Wallis, A. Adebisi, E. Nep, ... & K. Asare-Addo, (2020). The use of visible and UV dissolution imaging for the assessment of propranolol hydrochloride in liquisolid compacts of Sesamum radiatum gum. Journal of Drug Delivery Science and Technology, 101511.

[32] K. Etherson, C. Dunn, W. Matthews, H. Pamelund, C, Barragat, N. Sanderson, & M. McAllister (2020). An interlaboratory investigation of intrinsic dissolution rate determination using surface dissolution. European Journal of Pharmaceutics and Biopharmaceutics.

[33] M. A. Alhnan, T. C. Okwuosa, M. Sadia, K. W. Wan, W. Ahmed, & B. Arafat, (2016). Emergence of 3D printed dosage forms: opportunities and challenges. Pharmaceutical research, 33(8), 1817-1832.

[34] E. Prasad, M. T. Islam, D. J. Goodwin, A. J. Megarry, G. W. Halbert, A. J. Florence, & J. Robertson, (2019). Development of a hot-melt extrusion (HME) process to produce drug loaded Affinisol™ 15LV filaments for fused filament fabrication (FFF) 3D printing. Additive Manufacturing, 29, 100776.

[35] A. Melocchi, F. Parietti, G. Loreti, A. Maroni, A. Gazzaniga, & L. Zama, (2015). 3D printing by fused deposition modeling (FDM) of a swellable/erodible capsular device for oral pulsatile release of drugs. Journal of Drug Delivery Science and Technology, 30, 360-367.

[36] B. C. Sil, M. P. Alvarez, Y. Zhang, C. P. Kung, M. Hossain, F. Iliopoulos, et al. 3D-printed Franz type diffusion cells. International Journal of Cosmetic Science. 2018;40(6):604-9.

[37] G. Suarato, R. Spanò, R. Bertorelli, A. Diaspro, A. Athanassiou, and S. Surdo. 3D-Printed, Pocket-Size Diffusion Cells for Skin Permeation Investigation. In Multidisciplinary Digital Publishing Institute Proceedings. 2018: Vol. 2, No. 13, p. 945

[38] D. Ding, J. Pan, S.HYeo, VWagholikar, S.H. Lim, C. Wu, J.Y. Fuh, and L. Kang. A miniaturized device for biomembrane permeation analysis. Materials Science and Engineering C. 2019: 103, p.109772.

[39] A. C. Moffat, M. D. Osselton, B. Widdop, J. Watts. Clarke's Analysis of Drugs and Poisons London: Pharmaceutical Press; 2011 [4th:[Available from: www.new.medicinescomplete.com.

[40] A. Goyanes, A. B. Buanz, A. W. Basit, & S. Gaisford, (2014). Fused-filament 3D printing (3DP) for fabrication of tablets. International journal of pharmaceutics, 476(1-2), 88-92.

[41] J. Skowyra, K. Pietrzak, & M. A. Alhnan, (2015). Fabrication of extended-release patient-tailored prednisolone tablets via fused deposition modelling (FDM) 3D printing. European Journal of Pharmaceutical Sciences, 68, 11-17.

[42] A. Goyanes, A. B. Buanz, G. B. Hatton, S. Gaisford, & A. W. Basit, (2015). 3D printing of modified-release aminosalicylate (4-ASA and 5-ASA) tablets. European Journal of Pharmaceutics and Biopharmaceutics, 89, 157-162.

[43] F. Alexis (2005). Factors affecting the degradation and drug-release mechanism of poly (lactic acid) and poly [(lactic acid)-co-(glycolic acid)]. Polymer International, 54(1), 36-46.

[44] L. M. Galantucci, F. Lavecchia, & G. Percoco, (2009). Experimental study aiming to enhance the surface finish of fused deposition modeled parts. CIRP annals, 58(1), 189-192.

[45] G. Percoco, F. Lavecchia, & L. M. Galantucci, (2012). Compressive properties of FDM rapid prototypes treated with a low cost chemical finishing. Research Journal of Applied Sciences, Engineering and Technology, 4(19), 3838-3842.